Ecological Indicators 150 (2023) 110205

Contents lists available at ScienceDirect

Ecological Indicators

journal homepage: www.elsevier.com/locate/ecolind

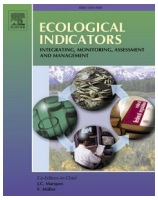

Geographic distribution, source analysis, and ecological risk assessment of PTEs in the topsoil of different land uses around the antimony tailings tank: A case study of Longwangchi tailings pond, Hunan, China

Hao Zou [a], Bozhi Ren [a,*], Xinping Deng [b], Tongshen Li [b]

[a] School of Civil Engineering, Hunan University of Science and Technology, Xiangtan 411201, China
[b] Hunan Geological Disaster Monitoring, Early Warning and Emergency Rescue Engineering Technology Research Center, Changsha 410004, China

ARTICLE INFO

Keywords:
Antimony tailings ponds
Topsoil
Source identification
Ecological risk assessment

ABSTRACT

Few studies have addressed the contamination of surface soils around antimony tailings ponds, and studying the contamination levels and sources of potentially toxic elements (PTEs) in soils around antimony tailings ponds and assessing the associated environmental risks are key steps in conducting environmental protection. Therefore, this study is the first to investigate the current status, spatial distribution, potential sources and ecological risks of Pb, Sb, Cr, Zn, Cd, As and Cu contamination in surface soils in woodlands, grasslands, farmlands and construction areas around the Longwangchi antimony tailings pond in Hunan, China. According to the analytic results of soil samples, the order of PTEs in terms of average concentration is: Sb > Zn > Cu > Pb > As > Cr > Cd. The cumulative index of land was applied to define Sb and Cd as extremely heavy pollution, and PLI divides the overall pollution level of soil into serious pollution levels. The ecological risk index was used to evaluate the risk characteristics of PTEs. The results showed that the ecological risk of Sb was particularly prominent, and 95% of the study area had reached a very high risk level. A quantitative comparison of ecological risk levels between different land uses revealed that there was a clear dividing line between regions, with built-up areas contributing the most to higher ecological risk at 8.89%, followed by 1.72% for grassland, 1.15% for agricultural land, and 0.57% for woodland. The visualization results of spatial distribution of PTEs exhibited that severe pollution occurred in the middle, north and southeast of the study area, and these distribution characteristics are mainly dictated by the polluted runoffs from tailings ponds and human activities. Principal component analysis (PCA) and positive matrix decomposition (PMF) were employed to identify the exact pollution sources, and the closer the determination coefficient (R^2) of PMF was to 1, the finer the pollution sources analyzed. A total of six potential sources of PTEs were analyzed by PMF: 36% of tailings pond contamination and mining operations, 8% atmospheric deposition, 19% traffic emissions, 9% combustion emissions, 11% natural sources, and 17% inputs related to agricultural production. This study is a complement to the study of environmental pollution around antimony tailing ponds, providing evaluation criteria for the pollution identification indicators of antimony tailing ponds.

1. Introduction

Antimony tailings ponding is an important derivative of antimony ore smelting, and a major contributor to the recovery of the large quantity of slag generated during the mining of antimony deposits (Chen et al., 2022). Sb and its related metals (Pb, Cd, etc.) in antimony tailings cause the concentration of PTEs in the tailings pond to rise to toxic levels, making the tailings pond the central area that precipitates pollution to the mine site (Davila et al., 2020). Since tailings and fine mud sediments in antimony tailings ponds are long exposed to complex chemical kinetic responses through external environmental change, they contain toxic heavy metals that enter nearby rivers and soils via groundwater seepage or surface runoffs (Kan et al., 2021), and the heavy metals that are lost enter the human body through soil, water and food chain transmission, posing a threat to health (Li et al., 2019). The pollution problems associated with tailings ponds have raised serious apprehension about the adverse impacts on the ecology, biodiversity and safety of the environment surrounding the ponds (Peša, 2021), and

* Corresponding author.
E-mail address: bozhiren@126.com (B. Ren).

https://doi.org/10.1016/j.ecolind.2023.110205
Received 17 January 2023; Received in revised form 28 March 2023; Accepted 29 March 2023
Available online 5 April 2023

have emerged as a critical issue of great concern and pressing need in environmental science.

In the survey of some tailing ponds, it is found that the concentration of heavy metal pollution is nearly 1000 times as high as the background value, presenting a grave threat to the local environment and ecology (Luo et al., 2021). Therefore, it is imperative for domestic and foreign scholars to evaluate the environmental pollution around the tailings pond (Liu et al., 2022). In terms of spatial distribution, in recent years, the assessment of soil pollution around tailings ponds via the geographical information system has attracted abundant attention (Xia et al., 2019, Xiang et al., 2019). Some scholars have analyzed the soil pollution brought about by Cu, U, Pb and Zn tailings ponds in Iranian and northwestern China through ordinary Kriging (OK) spatial interpolation method and inverse distance weight method (IDW), with an emphasis on the areas adjacent to the tailings basins. The results demonstrated that the pollution concentration often declined with tailings ponds as the center of dissemination: the closer the tailings pond, the deeper the degree of soil contamination, and the concentration of PTEs fell as the soil depth rose, which indicated that the pollution of topsoil by tailings ponds was much higher than that of deep soil (Chen et al., 2018, Khamseh et al., 2017, Yong et al., 2021).

Principal Component Analysis (PCA), Positive Matrix Factorization (PMF) and Hierarchical Cluster Analysis (HCA) have been extensively used in source analysis (Egbueri, 2020a, Nakagawa et al., 2020). For example, Wang and Hao et al. looked into PTEs sources in the environment surrounding several tailings ponds in Hubei and Guangdong, China, by means of PCA, HCA, and PMF, respectively, and found tailings ponds to be the primary cause of heavy metal contamination and that other sources were associated with tailings ponds and their relevant activities (Hao et al., 2022, Wang et al., 2022). Xiao et al. applied absolute Principal Component-Multiple Linear Analysis (APCS-MLR) to analyze the sources of heavy metals in soils around typical copper tailings ponds, and the authors concluded that tailings release was the main source of heavy metals in soils.(Xiao et al., 2022). Zhang et al. used PCA to identify the sources of potentially toxic elements in the soil around a gold tailing pond in China and found that the contamination mainly originated from the tailing pond, with some influence from agricultural activities (Zhang et al., 2021). The analysis of pollution sources around tailings pond is not limited to soil, Khademi et al., for instance, gleaned atmospheric dust from the environment surrounding tailings ponds in the southeastern Iberian Peninsula via dust collectors and dissected the sources of the PTE in it, with the conclusion that long-term exposed tailings surfaces and surface soils in the adjacent areas to tailings ponds were the major sources of PTE in the dust (Khademi et al., 2018). These results showed that the tailings ponds were not only the central pollution site but also a secondary source of potential damage to the surrounding environment.

When it comes to ecological risks, an increasing number of researchers are giving prominence to the risk of hazards posed by tailings ponds to their surrounding environment (Yin, 2023). The research of Mara et al. affords new directions for ecological risk assessment methodologies with regard to tailings ponds in Romanian counties through a generic approach for the identification of risks and the quantification of potential environmental impacts (Mara et al., 2007). The ecological risk index was adopted by Young and Zhang et al. to gauge the risk level of the soil environment around a gold and iron tailings pond in China, illustrating that the tailings pond constituted a high degree of ecological risk to the adjacent soil environment, since over half of the research area was characterized by a rather high risk score, while areas distant from the tailings pond displayed relatively little risk (Young et al., 2021, Zhang et al., 2021). Pollution resulting from tailings ponds is a primary factor in the high risks of the surrounding environment.

Multiple studies have shown that tailings ponds are causing increasing pollution to the surrounding soil environment, with greater contamination to surface soil than deep soil. To date, however, much research has been focused on managing environmental pollution in the surrounding environment of copper, iron, uranium and other tailings ponds. There's a lack of studies on the current status of topsoil contamination around antimony tailing ponds, with deficiencies still present in analyzing the physicochemical properties of PTEs in topsoil around antimony slag ponds and in assessing potential environmental risks, which can give rise to the spread of pollution over a larger area, thus bringing a range of negative impacts to the surrounding soils and ecosystems (Dusengemungu et al., 2022).

Xikuangshan in Lengshuijiang City, the world's largest antimony mine, is divided into the North Mine and South Mine, covering an area of about 70 km^2(Wu et al., 2011). The Longwangchi tailings pond is located in the northern part of the mine. To date, many studies have been conducted with respect to the area, such as contamination surveys of antimony mine soils, tailings, groundwater, aquatic plants and surrounding crops (Fu et al., 2010, He, 2007, Li et al., 2014, Qi et al., 2011). However, a probe into the pollution and hazards of antimony tailings ponds has not yet been launched. Efforts in this regard are vital because they involves aspects such as environmental safety and ecological risk to the soil around the antimony tailings ponds. Therefore, this study aims to expound and supplement the research on environmental pollution around antimony tailing ponds and provide effective suggestions for the environmental management of antimony tailing ponds in the future. The objectives of the present study are: (1) To investigate the levels and spatial distribution of 7 heavy metals (Cu, Zn, Sb, Cd, Pb, Cr, As) in topsoil surrounding tailings reservoirs. (2) To compare the accuracy of PCA and PMF statistical analysis methods and quantify the contribution of pollution sources to obtain accurate pollution sources; (3) To identify the potential ecological risk to the local area caused by soil contamination around the tailings ponds.

2. Research area and materials

2.1. Research area

The Longwangchi tailings pond is located in Lengshuijiang City, Hunan Province, China, and hailed as "the Antimony Capital of the World", as shown in Fig. 1. Its coordinates are 27°44′39 "N and 111°27′30 "E. Lengshuijiang pertains to a typical humid-hot monsoon subtropical climate zone, with warm summers and dry winters and distinct seasonal characteristics. The rainy season occurs mostly between April and June, with an average of 162.6 days of rainfall per year and an average annual rainfall of 1,159 mm. The average annual temperature is 18 °C, annual humidity 78%, the maximum temperature 40 °C and the minimum temperature −4 °C. There's a residential area and a high school in the east of the area, and several antimony smelting and processing enterprises in the central part, with County Road Z003 running through the southeastern section of the study area.

The site belongs to a tectonically denuded low hilly valley, and its original topography is undulating, with a steep terrain, mostly on hillsides. The Longwangchi tailings pond is situated in a valley between woodland and grassland, surrounded by original vegetation such as pine trees, and the dam is a permeable rockfill dam with a low topography. Over the years, due to the lack of environmental planning and environmental management, the tailings generated from mining, the abandoned heavy metal-containing slag and the slag of antimony-related enterprises are piled up haphazardly without any protective measures taken, and, as a result, a large number of harmful elements leach out during the rainy season, bringing about severe pollution to the environment around the pond.

2.2. Sample collection & analysis

A total of 349 topsoil samples were collected in the research area during the dry season in September 2021 and divided into four areas based on land uses: forest sampling site (82), grassland sampling site (67), farmland sampling site (72), and construction area sampling site

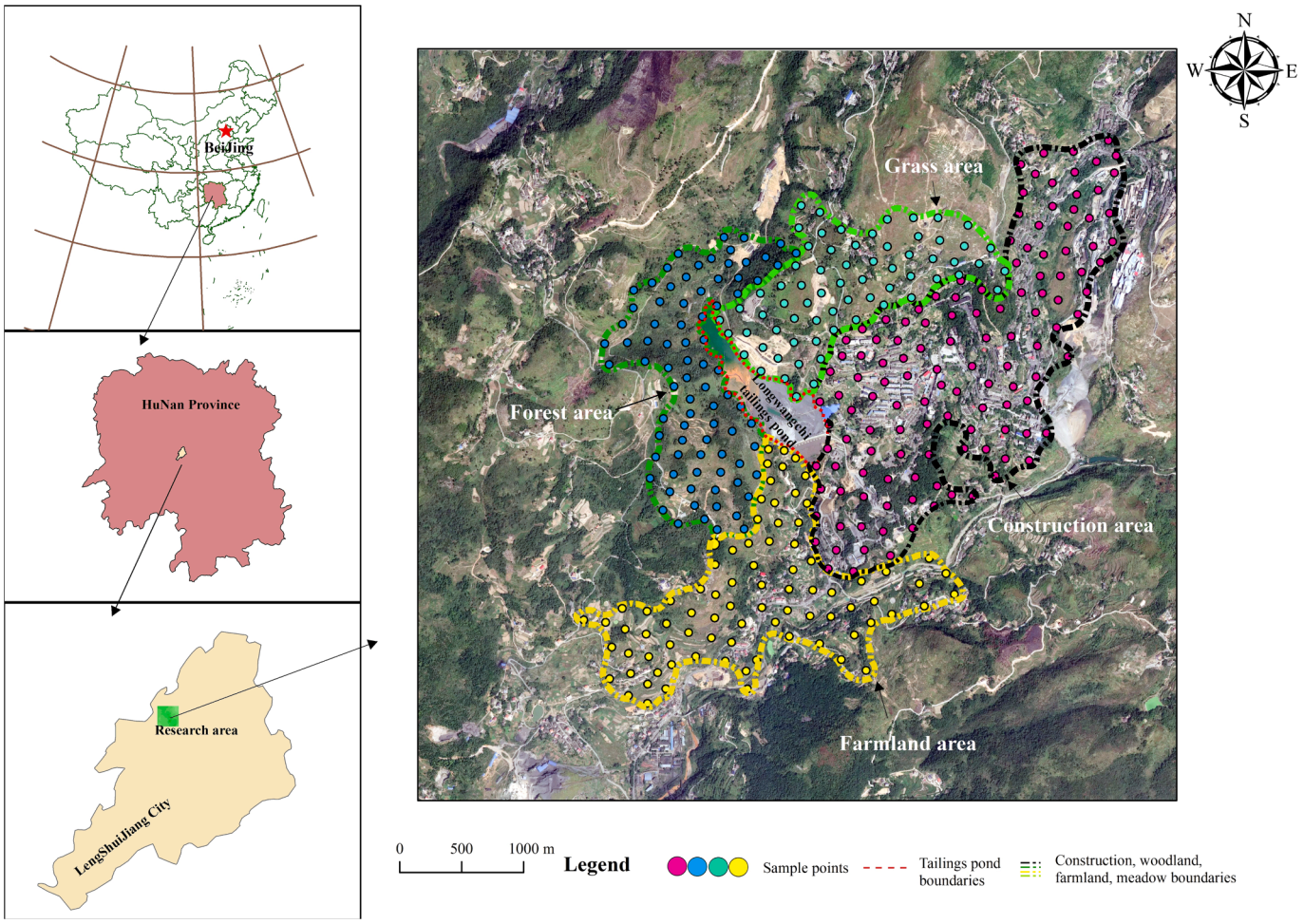

Fig. 1. Geographical location of the research area and distribution of sampling points.

(128) (see Fig. 1). The forest zone is mostly upland around the tailings pond, dominated by large numbers of plants and trees, and may not be affected by overland flows and atmospheric deposition. The agricultural area is primarily low-lying land, downstream of the tailings pond dam with a gentle slope, commonly subject to surface runoffs and farming activities. The grassland is mostly a high-elevation area near the tailings pond, principally influenced by agricultural activities and atmospheric deposition. The construction site is mainly a gently sloping field near the downstream end of the tailings pond dam, where antimony mining and smelting operations are highly concentrated, and are susceptible to surface runoffs, human activities as well as mining operations. The sampling followed the Technical Guidelines for Site Environmental Investigation (HJ25.1-2014) and the Technical Specification for Land Environment Monitoring (HJ/T166-2004), with the sampling depth being 0 to 50 cm of surface soil, using the grid-distribution method. Both manual and mechanical sampling were adopted, each consisting of 5 sub-samples taken from the center and four corners of the 100 m × 100 m region. The 1 kg of soil from each sampling site was numbered and brought to the laboratory in polyethylene sealed bags. The coordinates of the central sample from each location were measured using GPS. After removing foreign matter from the above soil samples, the large soil blocks were crushed and spread into a thin layer about 2 cm thick on a wooden plate for air drying. Then the ground samples were passed through a 100-mesh nylon screen, and the screened samples were all placed in polyethylene film (60 cm × 60 cm) for full mixing and even mixing. The processed samples were divided into two parts, one stored in the laboratory warehouse, the other for analysis. Accurately weigh 0.5 g of the soil sample in a polytetrafluoroethylene crucible, moisten it with a small amount of water and add 10 ml concentrated hydrochloric acid. Put the crucible on an electric heating plate and heat it at a low temperature. When it evaporates to about 5 ml remaining, add 15 ml concentrated nitric acid and continue heating until the solution is nearly viscous. Rinse the inner wall and the crucible cover with water, and dissolve the residue in warm heat. After cooling, the volume is fixed to 100 ml. For each sample, 10% parallel sample determination, full procedure blank testing and spike recovery determination were performed to ensure the quality and control standards of chemical analysis. The PTEs in the samples were leached out by horizontal shaking method and Cu, Zn, Cd, Pb, and Cr were determined by flame atomic absorption spectrometry (Wen et al., 2018), Sb and As were analyzed for concentration using graphite furnace atomic absorption spectrometry (Ren et al., 2015).

3. Analysis and evaluation methods

3.1. Statistical analysis

A matrix analysis of the Pearson correlation coefficient was performed on 7 types of PTEs from 349 samples using the SPSS package version 26.0 (IBM, SPSS Statistics, Chicago, IL, USA). The Pearson correlation coefficient is typically used to quantitatively assess the correlation between variables, thereby providing a valid basis for interpreting a variety of environmental factors (Zhao et al., 2022).

The contribution of PTEs from surface soil around the tailings reservoir was analyzed and compared via Positive Coefficient Matrix and Principal Component Analysis. PCA can efficiently identify and

detect PTE pollution sources in the environment. The main idea of PCA is dimensionality reduction, which allows large-scale datasets to be visualized (Chettri et al., 2022). PMF, as a receptor model for quantitative identification of key contaminants by analyzing the profile of sample data (Cheng et al., 2020), PMF improves the accuracy of source resolution by assigning an uncertainty to each valid data point (Xia et al., 2020). When the number of source factors obtained from PCA and PMF analysis is not uniform. To compare the accuracy of the two allocation methods, the coefficient of determination (R^2) was employed, and the closer R^2 was to 1 and the number of sources was appropriate, the greater the reliability of the method.

Previous studies have shown that most of the soils in the tin mining areas of Lengshuijiang City are contaminated from point sources (Xie and Ren, 2022). Considering the local concentration distribution of PTEs in soil, IDW was selected for geospatial analysis. The reason for this is that, in contrast to other interpolation methods, IDW can handle outliers (outliers) in the data set and predict the values of unknown regions in an integrated manner (Goix et al., 2013). PTEs were distributed spatially in Arcgis 10.8 software (ESRI, Redlands, California, USA).

3.2. Evaluation methodology

3.2.1. Geo-accumulation Indexes

Geo-accumulation Indexes (I_{geo}), serves as a means of assessing the level of accumulation of PTEs in sediments or other materials, taking into account the effect of differences between current and background concentrations(Jiang et al., 2020). In this study, equation (1) was employed to compute.

$$I_{geo} = \log_2(C_i/1.5B_i) \quad (1)$$

Where C_i is the content of element i and B_i is the environmental background value. In this paper, the environmental background value of Hunan Province in the Chinese Soil Elemental Background Value was chosen as the standard value. The constant 1.5 is often adopted as a factor and is intended to reflect the natural fluctuations of the background values (Egbueri et al., 2020). For example, the soil accumulation index can be broken down into 7 contamination categories (Kormoker et al., 2019): When $I_{geo} < 0$: No Contamination; $0 < I_{geo} < 1$: No to Moderate Contamination; $1 < I_{geo} < 2$: Moderate Contamination; $2 < I_{geo} < 3$: Moderate to Severe contamination; $3 < I_{geo} < 4$: Severe Contamination; $4 < I_{geo} < 5$: Severe to Very Severe Contamination; $I_{geo} > 5$: Very Heavy Contamination.

3.2.2. Enrichment factor (EF)

The enrichment factor is often used in various studies as a marker to distinguish natural from anthropogenic trace elements and to reflect the degree of trace element contamination of the soil. In this study, equation (2) was employed to compute.

$$EF = (C_i/C_R)_{sample}/(C_i/C_R)_{background} \quad (2)$$

$(C_i/C_R)_{sample}$ was adopted to study the ratio of elemental to reference concentrations, and $(C_i/C_R)_{background}$ used to study the ratio of geochemical background elemental concentrations to reference elemental values. The natural Al concentration tends to be homogenous, so Al was taken as the normalized element. EF was divided into 5 categories of contamination, $EF < 2$: slight man-made contamination; $2 < EF < 5$: moderate man-made contamination; $5 < EF < 20$: high man-made contamination; $EF > 40$: heavy man-made contamination (Sutherland 2000). If EF tends to 1, then there is no human influence, and the metal is likely to be of natural origin (Rashed 2010).

3.2.3. Pollution load index (PLI)

The PLI can reflect the overall contamination situation based on individual elements. The calculation formula is as follows:

$$CF_i = C_i/BV_i \quad (3)$$

$$PLI = (CF_1 \times CF_2 \times \bullet\bullet\bullet \times CF_n)^{1/n} \quad (4)$$

where CF_i denotes the contamination indicator of element i, C_i is the concentration of the element, and BV_i is the element's background. CF $\leq$ 1, 1–3, 3–6, >6 and PLI < 1, 1–2, 2–3, $\geq$3 are classified into four levels, indicating low, moderate, high, and severe pollution, respectively.

3.2.4. Eco-Risk index

Swedish academic Hakanson was the first to propose the potential ecological risk index. RI is often used to assess possible risk factors in the environment, such as soil, dust, sediment and water bodies (Egbueri and Enyigwe 2020). It is a simple and convenient method, with its computational formula seen as follows.

$$RI = \sum E_n^i = \sum T_n^i \times C_n/C_n^i \quad (5)$$

Where E_n^i is the potential ecological risk index of element i. C_n is the amount of PTEs in the samples. C_n^i is the background value of PTEs in soils of Hunan province, and T_n^i is the toxicity response factor. In this paper, the toxicity response factors of Cu, Pb, Zn, Cd, Cr and As were defined as 5, 5, 1, 2, 30 and 10, respectively (Egbueri, 2020b), and considering the similar geochemical behavior of Sb and Pb, the toxicity response factor of Sb is also defined as 5 (Krachler et al., 2005). The following Table 2 shows the basic hazard index levels.

4. Results

4.1. Pollution characteristics

The descriptive analysis of baseline PTE concentrations and parameters in the surrounding farmlands, woodlands, grasslands, buildings and the study area as a whole within the Longwangchi tailings pond are presented in Table 3. Regarding the enrichment factor, the overall EF value of Cr in the research area was <1. The result demonstrates that Cr originates from the crust and natural weathering. All of the anthropogenic effects of other heavy metals on pollution reached moderate ($2 < EF < 5$) or higher levels. Copper in grasslands, built-up areas and As in grasslands had EF values >5, all of which were highly anthropogenic in nature. In all areas, Cd and Sb reached heavy levels of anthropogenic pollution ($EF > 40$).

As far as the study area as a whole is concerned, the mean values of all PTEs concentrations except Cr were geometrically greater than the background concentrations, with a minimum of 3.25 times for As and a maximum of 205 times for Sb, signifying that some of the sampled soils were contaminated with Sb, As, Pb, Zn, Cd and Cu, with the chemical contamination of Sb being exceptionally conspicuous. In addition, the construction site was the most prominent area of contamination, where the average values of the concentrations of Zn, Cu, Sb, Pb reached the maximum. As the construction site, being the nearest to the downstream

Table 1
Pearson correlation coefficients of PTEs.

	Cr	Cd	Cu	Zn	Pb	Sb	As
Cr	1						
Cd	0.165[b]	1					
Cu	0.146[b]	0.430[b]	1				
Zn	0.231[b]	0.386[b]	**0.654**[b]	1			
Pb	0.172[b]	0.374[b]	**0.690**[b]	**0.831**[b]	1		
Sb	−0.174[b]	0.103	0.203[b]	0.119[a]	0.297[b]	1	
As	0.151[b]	0.098	0.090	0.037	−0.107	0.032	1

Note:
[a] indicates significant correlation at 0.01 level (2-tailed).
[b] indicates significant correlation at 0.05 level (2-tailed).

Table 2
Classification standards of potential ecological risk index.

Index	Ecological risk pollution level				
	Low Risk	Medium Risk	Higher Risk	High Risk	Very High Risk
E_r^i	$E_r^i < 40$	$40 \leq E_r^i < 80$	$80 \leq E_r^i < 160$	$160 \leq E_r^i < 320$	$E_r^i \geq 320$
RI	RI < 150	150 ≤ RI < 300	300 ≤ RI < 600	RI ≥ 600	

of the permeable fill dam of the tailing pond, was severely affected by the surface runoffs from the pond, and several antimony mining and smelting enterprises were clustered in the area, most of the Zn, Sb, Cu, Pb were obtained. The largest concentrations of arsenic were found in the grasslands, where large amounts of arsenic have accumulated due to agricultural activities and atmospheric deposition. Since the mean values of chromium concentrations in the topsoil of different lands were less than the background values, it was confirmed that chromium contamination may come from natural factors. In addition, it is worth noting that the concentrations of Sb and Cd in all samples were higher than their background values, and the study area was severely contaminated by Sb and Cd, which was also consistent with the results of previous studies in this area (Qi et al., 2022). The contamination of Sb and Cd is a problem that needs to be reckoned in the study area.

The coefficient of variation (CV) is often used as an indicator to determine the extent to which natural or external factors have a bearing on the content of each element in the soil. The weathering process of the soil parent material and the effects of human activities are highlighted by the effects of natural and external factors, respectively (Deng et al., 2019). When CV ≤ 20% means low impact, 21%<CV ≤ 50% means medium impact, 51%<CV ≤ 100% means high impact, CV > 100% is determined to be abnormally high impact (Qing et al., 2015). In the overall environment of the research area, the CVs for Cd, Cu, Zn and Pb were >100%, exhibiting an unusually high impact, and the CV for As and Sb were 85%, indicating a high impact. The coefficient for variation of Cr was 42%, that is, a moderate impact, smaller than those for the other elements. The most severe soil contamination occurred in the construction area, in which the CVs of Cd, Cu, Zn and Pb were >100%, with this of Zn and Pb as high as 262% and 314%, respectively, and the CV of Sb in the buildings area also peaked at 93%, signifying that human activities exerted a powerful influence on the concentration of PTEs in this region. The high variability of Cd, Cu, Zn, Pb, As, and Sb, construed in terms of coefficient of variation, points to the influence of external factors in the introduction of these elements.

In the research area, the mean magnitude of I_{geo} of PTEs was in the following order: Sb (7.10) > Cd (5.43) > Cu (1.54) > Pb (1.41) > As (1.12) > Zn (1.01) > Cr (−1.09). Among them, Sb has reached the level of serious pollution in different types of land uses, and the pollution level of Sb in the study area is much higher than that in Qinglong antimony tailings in Guizhou and other areas of Xikuangshan (Li et al., 2023, Luo et al., 2021). As was moderate pollution in woodlands and grasslands, and non-pollution to moderate pollution in construction and farmland areas. Cu, Zn, Pb were mostly concentrated in the construction area and all achieved moderate levels of pollution, whereas they were non-pollution to moderate pollution in other land uses. There was no Cr contamination in the research area. Fig. 2 shows the contribution of the I_{geo} distribution range of PTEs, and it can be seen that the distribution of the rank contributions of Cu, Zn, Pb, As to the I_{geo} values is very similar, which suggests that the effects of human activities and natural geological effects may have the same effect on them. A small number of non-normal values of Cu, Zn, and Pb in the sample were classified as heavy to very heavy contamination or heavy pollution, i.e., these sites were contaminated by point sources (Liu et al., 2021).

Table 3
Descriptive analysis of PTEs in soil (including the research area as a whole and areas with different land use types) (mg/kg).

Element	Regional Classification	Min/Max	Mean ± S.D	Coefficient of variation (%)	Background value	EF	I_{geo}
Cu	Forest area	14/263	62.92 ± 56.09	89	27.3	2.31	0.62
Zn		51.2/568	253.34 ± 178.19	70	94.4	2.68	0.84
Cd		0.51/27.52	8.31 ± 7.99	96	0.126	65.98	5.46
Pb		20.8/122.5	69.32 ± 32.83	47	29.7	2.33	0.64
Cr		24.6/93	57.76 ± 15.59	27	71.4	0.81	−0.89
As		20.1/133	55.85 ± 34.73	62	15.7	3.56	1.25
Sb		26.6/708	331.42 ± 182.13	55	1.87	177.23	6.89
Cu	Grass area	16.3/361	151.08 ± 118.48	64	27.3	5.5	0.91
Zn		44.6/835	266.66 ± 170.13	90	94.4	2.91	0.96
Cd		0.32/53.36	8.65 ± 9.77	113	0.126	68.63	5.52
Pb		16.8/359	86.42 ± 77.89	90	29.7	2.91	0.96
Cr		16.6/99	56.59 ± 24.81	44	71.4	0.79	−0.92
As		9.88/281	88.25 ± 65.95	75	15.7	5.62	1.91
Sb		8.63/863	279.98 ± 225.64	81	1.87	149.72	6.64
Cu	Construction area	12/2300	171.79 ± 224.97	131	27.3	6.30	2.07
Zn		28/8770	303.73 ± 795.60	262	94.4	3.22	1.10
Cd		0.35/70.3	7.26 ± 9.63	133	0.126	57.63	5.26
Pb		16.8/4430	133.96 ± 421.10	314	29.7	4.51	1.59
Cr		14/123	47.92 ± 21.46	45	71.4	0.67	−1.16
As		12.5/136	41.84 ± 27.71	66	15.7	2.67	0.83
Sb		19.5/2170	471.50 ± 436.00	93	1.87	252.14	7.39
Cu	Farmland area	14.6/280.9	55.03 ± 59.73	109	27.3	2.02	0.43
Zn		56.2/984	206.54 ± 194.02	94	94.4	2.19	0.55
Cd		0.29/17.64	8.90 ± 4.83	54	0.126	70.65	5.56
Pb		18.6/131	74.56 ± 34.18	46	29.7	2.51	0.74
Cr		20.9/74.3	41.92 ± 17.71	42	71.4	0.59	−1.35
As		7.69/68	27.84 ± 15.54	56	15.7	2.01	0.24
Sb		18.3/842	267.69 ± 216.62	81	1.87	143.15	6.58
Cu	Overall	12/2300	118.80 ± 160.33	135	27.3	4.35	1.54
Zn		44.6/8770	283.61 ± 509.77	180	94.4	3.00	1.01
Cd		0.29/70.3	8.14 ± 8.56	105	0.126	64.71	5.43
Pb		16.8/4430	117.98 ± 265.44	225	29.7	3.97	1.41
Cr		14/123	50.46 ± 21.09	42	71.4	0.71	−1.09
As		7.69/281	51.06 ± 43.34	85	15.7	3.25	1.12
Sb		8.36/2170	383.71 ± 324.73	85	1.87	205.20	7.10

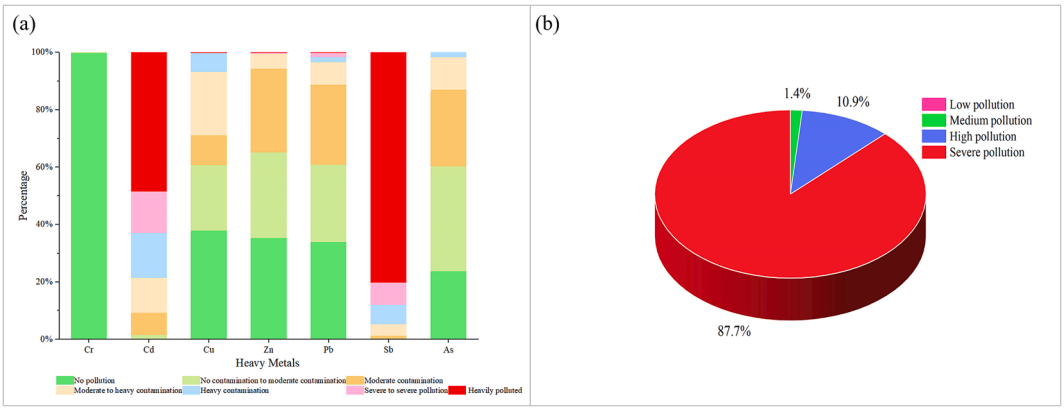

Fig. 2. (a) Heavy metal element I_{geo} range distribution proportion map, (b) PLI range distribution.

The overall pollution of soil samples can be classified according to PLI (see Fig. 2(b)). In this study, the PLI values ranged from 1.59 to 51.48, with a mean value of 5.45. The distribution of soil pollution levels is as follows: no low-level pollution points, and the sampling points with moderate pollution account for 1.4%, while the high pollution and heavy pollution account for 10.9% and 87.7% respectively. The overall soil contamination level in the study area was defined as severe based on the overall contamination reflected by PLI.

4.2. *Geospatial distribution of heavy metals around tailings ponds*

Geospatial distribution of PTEs in soils can provide useful information for research, such as sources of elements and possible enrichment zones (Fei et al., 2019), Understanding the geospatial distribution of these elements is pivotal for tackling problems such as accumulation of soil PTEs and anthropogenic influences (Bai et al., 2016). The geospatial distribution information of PTEs acquired using the IDW method is shown in Fig. 3. Cr was free from human interference and constituted no environmental pollution in the study area. It was therefore not applied to the visualization of ArcGIS.

From Fig. 3, the areas with high contents of Cu, Zn, Cd, Sb, Pb were similarly distributed in the middle of the research area near the southeast, where the terrain was low and more gentle, and these areas were by and large situated downstream of the tailings ponds, agricultural land, and construction areas. High As values occurred in the north of the research area, near the high- elevation woodlands and grasslands. According to the spatial distribution and field investigation of heavy metals, it can be found that: Firstly, contaminated run-off from tailings ponds and mining production was the most direct route for PTE to penetrate into the soil. There were more than thirty antimony mining companies in the central region engaged in the processing and smelting of antimony ore, and the waste, tailings and slag from the high-input antimony mines, as well as the wastewater from the production of antimony and metals, were concentrated in the permeable embankment of the Longwangchi fine mud tailings reservoir. Previous investigations have illustrated that one characteristic of PTEs deposits in tailings ponds was that they mixed easily with water flow, and when the proportion of PTEs present in the substrate was high, more PTEs accumulated in the soil near the tailings ponds and in low-lying areas (Yuan et al., 2018), thereby penetrating farmlands and surface water and spreading into surrounding areas. Moreover, the high enrichment of PTEs in the central and southeastern parts of the study area was also attributed to the use of

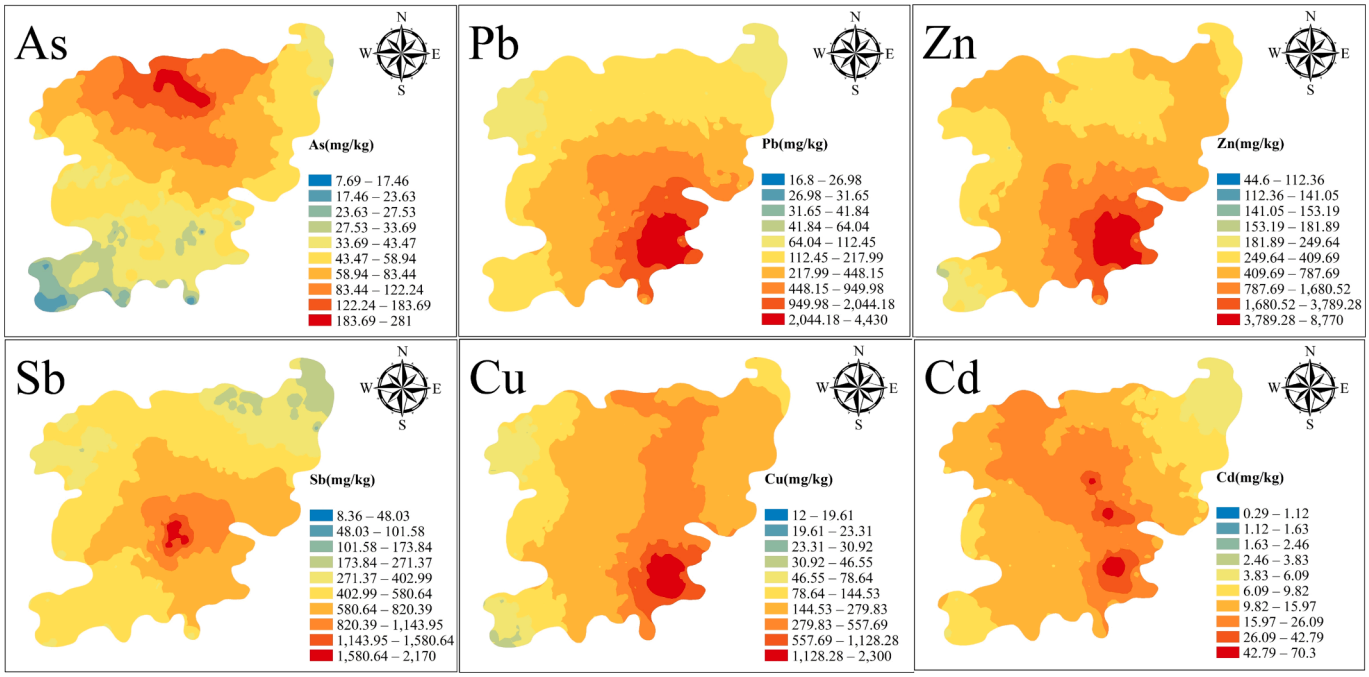

Fig. 3. Spatial distribution of PTEs other than Cr.

PTE-bearing deposits and substrates by residents to fill the open space.

Secondly, vehicular traffic due to mining activities and tailings accumulation also contributes significantly to the convergence of PTEs in the area. Since the commissioning of the Longwangchi tailings pond in 1983, the distribution of PTE in the study area has been affected by pollution from vehicle transportation caused by tailings build-up for almost 40 years. County-Road Z003 passes through the southeast side of the study area and is frequently used by vehicles as a major arteryfor the transportation of tailings. Yang et al. argued that vehicular traffic from years of mining activities had boosted Cu, Zn, and Pb enrichment at the mine site (Yang et al., 2016).

Thirdly, agricultural activities may also have a bearing on soil PTE distribution. Agricultural activities, including the use of fertilizers, pesticides, and herbicides by residents, and the transportation of soil from agricultural fields or upslope from tailings ponds to downstream or downslope areas in order to enhance soil fertility, offer crucial evidence for anthropogenic influence. At the same time, depending on the nature and distribution of local soil, this area is clay in texture, with a high adsorption capacity, Thus, heavy metals from fertilizers, pesticides and herbicides build up in the soil, and may be transmitted with anthropogenic activities, resulting in contamination of the surface soil surrounding the tailings pond.

4.3. Source analysis

The correlation between PTEs in the study area was explored using the Pearson correlation coefficient matrix (Table 1). Zn boasted the highest correlation with Pb ($r^2 = 0.831$), followed by Cu and Pb($r^2 = 0.690$), and then Cu and Zn ($r^2 = 0.654$), respectively, while the degrees to which Cr, Cd, Sb, and As were correlated were not high. Higher item correlations generally indicate that items may have the same origin or similar laws of movement and pathways throughout the study region, whereas smaller or even negative correlations demonstrate that items tend to have divergent origins (Li et al., 2017).

The sources of PTEs in the study area were categorized using PCA and PMF methods, respectively, and their respective contribution rates were quantified (Fig. 4). Three principal components were extracted by PCA, which were capable of accounting for approximately 74% of the variance. The agreement between measured and fitted concentrations was checked according to the coefficient of determination (R^2) (Table 4), since the results showed that R^2 was closer to 1 on the PMF model and the PMF displayed better performance. In consequence, PMF was used as the receptor model for source identification in this paper.

This study utilized EPA PMF 5.0 (USEPA, USA) to decompose the data to obtain possible sources. The input model concentration and uncertainty data were subjected to twenty factor iterations respectively in an effort to improve the accuracy of the prediction. (Wu et al., 2021). The optimal solution could be found when the number of source factors was fixed at 6. Cu (88.3%) was the dominant element in factor 1. It is likely that the contribution to Cu stemmed directly from the influence of contaminated runoffs from the antimony tailings pond, where large numbers of heavy metals were delivered to the soil surrounding the tailings pond via runoffs (Du et al., 2015). In addition, the results of previous studies have shown that tire and brake lining wear contribute significantly to Cu (Zhang et al., 2016). Cd was the second factor, representing 90.3%. From an enrichment factor perspective, the greater Cd accumulation was anthropogenic in origin (Xiao et al., 2021). Cd was primarily produced by municipal sewage, agricultural production, and atmospheric deposition (Rehman et al., 2018). Fertilizer and pesticide applications also played a vital role in the buildup of Cd in soils. Cr contributed 88.4% to the 3-factor. The concentration of Cr always fluctuated with background value. Compared with other heavy elements, Cr had an EF value lower than 1. It was minimally affected by anthropogenic perturbations. Natural rock weathering and soil erosion dominated Cr sources. In factor 4, Sb comprised 85.9% of the total. The mining of the antimony deposits for over 110 years and the accumulation of large quantities of antimony-containing tailings have wreaked much havoc on the local environment. The findings of the site survey suggest that the exposed Sb-rich mine waste in tailings ponds has

Table 4
R^2 of PCA and PMF methods.

R^2	Cr	Cd	Cu	Zn	Pb	Sb	As
PCA	0.663	0.397	0.716	0.810	0.851	0.747	0.918
PMF	0.989	0.999	0.944	0.926	0.809	0.999	0.951

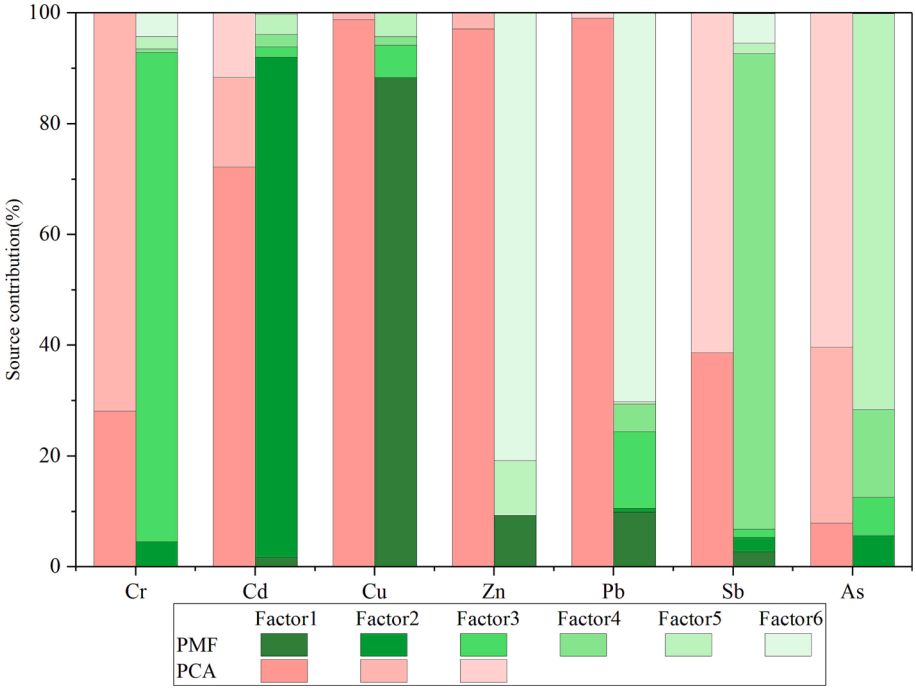

Fig. 4. Contribution of PMF and PCA to the identification of possible sources.

become a direct source of Sb contamination, and that mine waste is located on slopes at higher altitudes, which can readily transfer Sb to surrounding soils and downslope soils in the wake of leaching or water weathering (Yang et al., 2018). Factor 5 contains 71.5% As, with the high concentration being primarily in the grass zone. Prior studies make it clear that the irrational use of herbicides, pesticides, and fertilizers can prompt As to accumulate in the soil (Xiao et al., 2019). Furthermore, As in the melting of dust particles deposited on the molten surface of slag waste and tailings that have been exposed for a long period of time in tailings ponds, atmospheric deposition can precipitate high levels of contamination of the surrounding soil (Sun et al., 2021). The surrounding woodlands are covered in dense vegetation which blocks atmospheric particulates, thus making grass the primary receiving area (Anaman et al., 2022). In factor 6, Zn (80.8%) and Pb (70.2%) act as the main contributors. Previous studies have verified the presence of abundant Zn in dust generated at the surface of tires and during rubbing (Apeagyei et al., 2011). Pb is mainly released from leaded gasoline (Liang et al., 2016).The use of leaded petrol has been banned in China since 2000, but the effects of transport-induced soil contamination from long-term antimony mining, smelting, and the accumulation of tailings ponds persist. However, the high correlation of Cu, Zn, and Pb cannot rule out the possibility that their sources are all linked to polluted runoffs from the tailing ponds.

Overall, the major sources of PTE in the region are 36% pollution and mining activities of tailings ponds, 8% atmospheric deposition, 19% traffic emissions, 9% combustion emissions, 11% natural sources and 17% input of agricultural production. Among them, tailings pond pollution and mining activities are the dominant causes affecting the environment around Longwangchi. The source of Sb in this study differs from those found previously in antimony mining areas in that the Sb in the study area arises directly from the transfer of antimony tailings and mine waste, rather than from atmospheric deposition from smelters as previous studies have shown (He et al., 2021, Sheng et al., 2022).

4.4. Ecological risk assessment

The mean E_n^i values of Cr、Cu、Zn、Pb and As in the research area are below 40 (see Fig. 5). It is advised that the ecological hazards posed by these elements in the research area should not be a prominent concern for future planning of environmental management and pollution prevention in the region. The mean values for Cd and Sb are 129.42 and 966.71, respectively, and Sb attains a very high-risk level, presenting a grave threat to the ecosystem.

Fig. 5 shows the distribution of RI values for forest, grassland, agricultural land, and built-up areas. The highest risk percentage (RI > 300) is found in built-up areas at 8.89%, followed by 1.72% in grasslands, 1.15% in farmlands, and the lowest at 0.57% in forested areas. A review of the geographical distribution of RI values illustrates that there are notable lines of demarcation of RI indices between the distinct land types (Hossain Bhuiyan et al., 2021). The construction areas are a major contributor to the higher ecological risk, which is closely associated with the long-term mining activities in the region. High-intensity mining has resulted in severe heavy metal contamination, especially the disposal of slag waste involving antimony and other metals and the discharge of wastewater containing antimony.

Fig. 6 features the spatial visualization of RI throughout the research area and Sb. Nearly the entire region is at a very high risk of Sb, and the research area is heavily contaminated with Sb, which becomes the primary driver of high ecological risk, resulting in a spatial distribution of RI across the study area that is very similar to that of Sb. Unlike this paper, previous studies concerning ecological risk in antimony mining sites have deemed Cd as the element with the highest ecological risk, and Sb much less toxic than Cd (Qi et al., 2022, Zhu et al., 2018). The finding of this study can be combined with existing research to supplement the risk assessment of the environment around the antimony tailings ponds, and, by incorporating local environmental factors, to provide a theoretical basis for the prevention effort of tailing pond pollution in the future.

5. Conclusion

Despite the issue of soil contamination in the vicinity of tailings ponds looming large, there are few studies concerned with the pollution induced by antimony tailings ponds. This study aims to investigate the contamination, distribution, sources and ecological risks of Cu, Zn, Sb, Cd, Pb, Cr and As in the surface soils of different land uses around the Longwangchi tailings pond in Xikuangshan, the “Antimony capital of the world”, Hunan Province, China, to determine the pollution potential of PTEs in the region, and to afford insights into the study of antimony tailings pond pollution. Proceeding from the overall findings, this paper presents the following highlights:

(1) The average concentrations of heavy metal elements except Cr exceed the background values. Sb is the main pollution element, and its average concentration is 205 times of the background value. The Sb and Cd are defined as severe pollution by I_{geo}, and PLI divides the overall pollution level of soil into serious pollution levels.
(2) In terms of enrichment factors, Cu, Zn, Pb and As are moderate anthropogenic pollution, and Sb and Cd fall under severe anthropogenic pollution.
(3) The results of source analysis show that Cr is a natural pollution source, while Cu, As, Cd, Sb, Pb and Zn are all man-made pollution sources.
(4) As far as ecological risks are concerned, differences in land boundaries give rise to differences in risks, with the construction areas identified as the dominant contributor to levels. Cd is no longer the element that causes the highest ecological risk, but the ecological risk of Sb is obvious. The pollution arising from mining

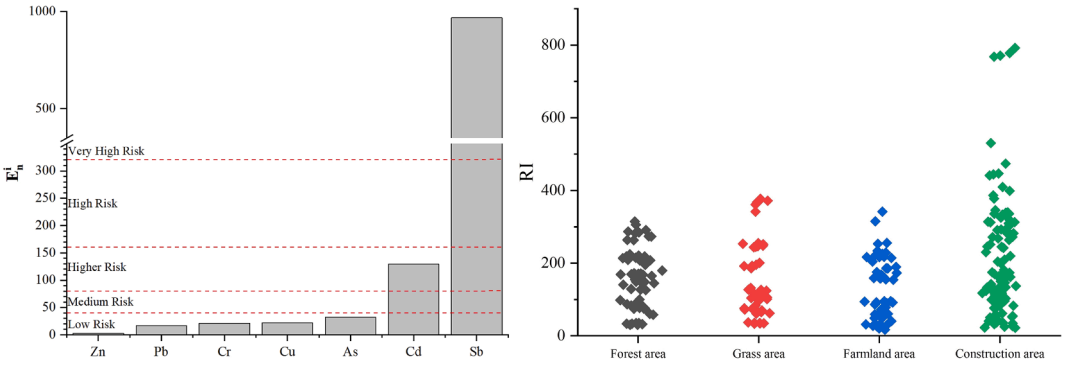

Fig. 5. Distribution of the ecological risk index and the range of RI values for woodland, grassland, agricultural land and built-up areas for each element.

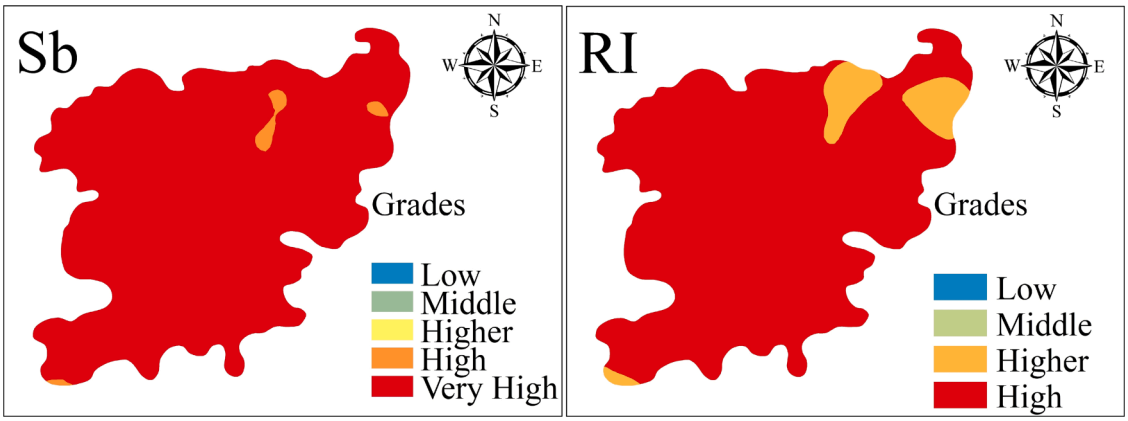

Fig. 6. Sb elements and ecological risk indicators in the study area.

activities and tailing ponds is the principal reason for the great ecological risk in the vicinity of the Longwangchi tailing pond.

This study complements the investigation of soil contamination around antimony tailing ponds, which can provide a solid theoretical basis for future environmental risk control around antimony tailing ponds and other aspects, and crystallize the priorities for subsequent pollution prevention efforts in tailing ponds. However, further comprehensive studies on the health risks of the environment around antimony tailing ponds are needed so as to establish a complete evaluation system for the risk studies of antimony tailing ponds.

CRediT authorship contribution statement

Hao Zou: Methodology, Writing – original draft, Investigation. **Bozhi Ren:** Conceptualization, Supervision. **Xinping Deng:** Investigation, Resources. **Tongshen Li:** Investigation, Resources.

Declaration of Competing Interest

The authors declare that they have no known competing financial interests or personal relationships that could have appeared to influence the work reported in this paper.

Data availability

Data will be made available on request.

Acknowledgements

This paper was funded by the National Natural Science Foundation of China (Project No. 41973078) and the Key R&D Project of Hunan Provincial Science and Technology Department (Project No. 2022SK2073).

References

Anaman, R., Peng, C., Jiang, Z., Liu, X., Zhou, Z., Guo, Z., Xiao, X., 2022. Identifying sources and transport routes of heavy metals in soil with different land uses around a smelting site by GIS based PCA and PMF. Sci. Total Environ. 823, 153759 https://doi.org/10.1016/j.scitotenv.2022.153759.

Apeagyei, E., Bank, M.S., Spengler, J.D., 2011. Distribution of heavy metals in road dust along an urban-rural gradient in Massachusetts. Atmos. Environ. 45 (13), 2310–2323. https://doi.org/10.1016/j.atmosenv.2010.11.015.

Bai, Y., Wang, M., Peng, C., Alatalo, J.M., 2016. Impacts of urbanization on the distribution of heavy metals in soils along the Huangpu River, the drinking water source for Shanghai. Environ. Sci. Pollut. Res. 23 (6), 5222–5231. https://doi.org/10.1007/s11356-015-5745-3.

Chen, Y., Hong, Y., Huang, D., Dai, X., Zhang, M., Liu, Y., Xu, Z., 2022. Risk assessment management and emergency plan for uranium tailings pond. J. Radiat. Res. Appl. Sci. 15 (3), 83–90. https://doi.org/10.1016/j.jrras.2022.06.005.

Chen, T., Lei, C., Yan, B., Li, L.-l., Xu, D.-M., Ying, G.-G., 2018. Spatial distribution and environmental implications of heavy metals in typical lead (Pb)-zinc (Zn) mine tailings impoundments in Guangdong Province, South China. Environ. Sci. Pollut. Res. 25 (36), 36702–36711. https://doi.org/10.1007/s11356-018-3493-x.

Cheng, W., Lei, S., Bian, Z., Zhao, Y., Li, Y., Gan, Y., 2020. Geographic distribution of heavy metals and identification of their sources in soils near large, open-pit coal mines using positive matrix factorization. J. Hazard. Mater. 387, 121666 https://doi.org/10.1016/j.jhazmat.2019.121666.

Chettri, U., Chakrabarty, T.K., Joshi, S.R., 2022. Pollution index assessment of surface water and sediment quality with reference to heavy metals in Teesta River in Eastern Himalayan range, India. Environ. Nanotechnol. 18, 100742. https://doi.org/10.1016/j.enmm.2022.100742.

Davila, R.B., Fontes, M.P.F., Pacheco, A.A., Ferreira, M.D.S., 2020. Heavy metals in iron ore tailings and floodplain soils affected by the Samarco dam collapse in Brazil. Sci. Total Environ. 709, 136151 https://doi.org/10.1016/j.scitotenv.2019.136151.

Deng, Y., Jiang, L., Xu, L., Hao, X., Zhang, S., Xu, M., Zhu, P., Fu, S., Liang, Y., Yin, H., Liu, X., Bai, L., Jiang, H., Liu, H., 2019. Spatial distribution and risk assessment of heavy metals in contaminated paddy fields - A case study in Xiangtan City. Ecotoxicol. Environ. Saf. 171, 281–289. https://doi.org/10.1016/j.ecoenv.2018.12.060.

Du, P., Xie, Y., Wang, S., Zhao, H., Zhang, Z., Wu, B., Li, F., 2015. Potential sources of and ecological risks from heavy metals in agricultural soils. Environ. Sci. Pollut. Res. 22 (5), 3498–3507. https://doi.org/10.1007/s11356-014-3532-1.

Dusengemungu, L., Mubemba, B., Gwanama, C., 2022. Evaluation of heavy metal contamination in copper mine tailing soils of Kitwe and Mufulira, Zambia, for reclamation prospects. Sci. Rep. 12 (1) https://doi.org/10.1038/s41598-022-15458-2.

Egbueri, J.C., 2020a. Groundwater quality assessment using pollution index of groundwater (PIG), ecological risk index (ERI) and hierarchical cluster analysis (HCA): a case study. Groundw. Sustain. Dev. 10, 100292. https://doi.org/10.1016/j.gsd.2019.100292.

Egbueri, J.C., 2020b. Heavy metals pollution source identification and probabilistic health risk assessment of shallow groundwater in Onitsha, Nigeria. Anal. Lett. 53 (10), 1620–1638. https://doi.org/10.1080/00032719.2020.1712606.

Egbueri, J.C., Enyigwe, M.T., 2020. Pollution and ecological risk assessment of potentially toxic elements in natural waters from the Ameka Metallogenic district in Southeastern Nigeria. Anal. Lett. 53 (17), 2812–2839. https://doi.org/10.1080/00032719.2020.1759616.

Egbueri, J.C., Ukah, B.U., Ubido, O.E., Unigwe, C.O., 2020. A chemometric approach to source apportionment, ecological and health risk assessment of heavy metals in industrial soils from southwestern Nigeria. Int. J. Environ. Anal. Chem. 102 (14), 3399–3417. https://doi.org/10.1080/03067319.2020.1769615.

Fei, X., Christakos, G., Xiao, R., Ren, Z., Liu, Y., Lv, X., 2019. Improved heavy metal mapping and pollution source apportionment in Shanghai City soils using auxiliary information. Sci. Total Environ. 661, 168–177. https://doi.org/10.1016/j.scitotenv.2019.01.149.

Fu, Z., Wu, F., Amarasiriwardena, D., Mo, C., Liu, B., Zhu, J., Deng, Q., Liao, H., 2010. Antimony, arsenic and mercury in the aquatic environment and fish in a large antimony mining area in Hunan, China. Sci. Total Environ. 408 (16), 3403–3410. https://doi.org/10.1016/j.scitotenv.2010.04.031.

Goix, S., Resongles, E., Point, D., Oliva, P., Duprey, J.L., de la Galvez, E., Ugarte, L., Huayta, C., Prunier, J., Zouiten, C., Gardon, J., 2013. Transplantation of epiphytic bioaccumulators (Tillandsia capillaris) for high spatial resolution biomonitoring of trace elements and point sources deconvolution in a complex mining/smelting urban context. Atmos. Environ. 80, 330–341. https://doi.org/10.1016/j.atmosenv.2013.08.011.

Hao, X., Yi, X., Dang, Z., Liang, Y., 2022. Heavy metal sources, contamination and risk assessment in legacy Pb/Zn mining tailings area: field soil and simulated rainfall. Bull. Environ. Contam. Toxicol. 109 (4), 636–642. https://doi.org/10.1007/s00128-022-03555-x.

He, M., 2007. Distribution and phytoavailability of antimony at an antimony mining and smelting area, Hunan, China. Environ. Geochem. Health 29 (3), 209–219. https://doi.org/10.1007/s10653-006-9066-9.

He, Y., Han, Z., Wu, F., Xiong, J., Gu, S., Wu, P., 2021. Spatial Distribution and environmental risk of arsenic and antimony in soil around an antimony smelter of

Qinglong County. Bull. Environ. Contam. Toxicol. 107 (6), 1043–1052. https://doi.org/10.1007/s00128-021-03118-6.
Hossain Bhuiyan, M.A., Chandra Karmaker, S., Bodrud-Doza, M., Rakib, M.A., Saha, B.B., 2021. Enrichment, sources and ecological risk mapping of heavy metals in agricultural soils of dhaka district employing SOM, PMF and GIS methods. Chemosphere 263, 128339. https://doi.org/10.1016/j.chemosphere.2020.128339.
Jiang, F., Ren, B., Hursthouse, A., Deng, R., 2020. Evaluating health risk indicators for PTE exposure in the food chain: evidence from a thallium mine area. Environ. Sci. Pollut. Res. 27 (19), 23686–23694. https://doi.org/10.1007/s11356-020-08733-0.
Kan, X., Dong, Y., Feng, L., Zhou, M., Hou, H., 2021. Contamination and health risk assessment of heavy metals in China's lead-zinc mine tailings: a meta-analysis. Chemosphere 267, 128909. https://doi.org/10.1016/j.chemosphere.2020.128909.
Khademi, H., Abbaspour, A., Martínez-Martínez, S., Gabarrón, M., Shahrokh, V., Faz, A., Acosta, J.A., 2018. Provenance and environmental risk of windblown materials from mine tailing ponds. Environ. Pollut. 241, 432–440. https://doi.org/10.1016/j.envpol.2018.05.084.
Khamseh, A., Shahbazi, F., Oustan, S., Najafi, N., Davatgar, N., 2017. Impact of tailings dam failure on spatial features of copper contamination (Mazraeh mine area, Iran). Arab. J. Geosci. 10 (11) https://doi.org/10.1007/s12517-017-3040-y.
Kormoker, T., Proshad, R., Islam, S., Ahmed, S., Chandra, K., Uddin, M., Rahman, M., 2019. Toxic metals in agricultural soils near the industrial areas of Bangladesh: ecological and human health risk assessment. Toxin Rev. 40 (4), 1135–1154. https://doi.org/10.1080/15569543.2019.1650777.
Krachler, M., Zheng, J., Koerner, R., Zdanowicz, C., Fisher, D., Shotyk, W., 2005. Increasing atmospheric antimony contamination in the northern hemisphere: snow and ice evidence from Devon Island, Arctic Canada. J. Environ. Monit. 7 (12), 1169–1176. https://doi.org/10.1039/b509373b.
Li, Y., Fang, F., Lin, Y., Wang, Y., Kuang, Y., Wu, M., 2019. Heavy metal contamination and health risks of indoor dust around Xinqiao Mining Area, Tongling, China. Hum. Ecol. Risk Assess. Int. J. 26 (1), 46–56. https://doi.org/10.1080/10807039.2018.1503930.
Li, X., Tang, Y., Wang, X., Song, X., Yang, J., 2023. Heavy metals in soil around a typical antimony mine area of China: pollution characteristics, land cover influence and source identification. Int. J. Environ. Res. Public Health 20 (3), 2177. https://doi.org/10.3390/ijerph20032177.
Li, J., Wei, Y., Zhao, L., Zhang, J., Shangguan, Y., Li, F., Hou, H., 2014. Bioaccessibility of antimony and arsenic in highly polluted soils of the mine area and health risk assessment associated with oral ingestion exposure. Ecotoxicol. Environ. Saf. 110, 308–315. https://doi.org/10.1016/j.ecoenv.2014.09.009.
Li, X., Yang, H., Zhang, C., Zeng, G., Liu, Y., Xu, W., Wu, Y., Lan, S., 2017. Spatial distribution and transport characteristics of heavy metals around an antimony mine area in central China. Chemosphere 170, 17–24. https://doi.org/10.1016/j.chemosphere.2016.12.011.
Liang, J., Liu, J., Yuan, X., Zeng, G., Yuan, Y., Wu, H., Li, F., 2016. A method for heavy metal exposure risk assessment to migratory herbivorous birds and identification of priority pollutants/areas in wetlands. Environ. Sci. Pollut. Res. Int. 23 (12), 11806–11813. https://doi.org/10.1007/s11356-016-6372-3.
Liu, S., Yuan, R., Wang, X., Yan, Z., 2022. Soil tungsten contamination and health risk assessment of an abandoned tungsten mine site. Sci. Total Environ. 852, 158461 https://doi.org/10.1016/j.scitotenv.2022.158461.
Liu, H., Zhang, Y., Yang, J., Wang, H., Li, Y., Shi, Y., Li, D., Holm, P.E., Ou, Q., Hu, W., 2021. Quantitative source apportionment, risk assessment and distribution of heavy metals in agricultural soils from southern Shandong Peninsula of China. Sci. Total Environ. 767, 144879 https://doi.org/10.1016/j.scitotenv.2020.144879.
Luo, G., Han, Z., Xiong, J., He, Y., Liao, J., Wu, P., 2021. Heavy metal pollution and ecological risk assessment of tailings in the Qinglong Dachang antimony mine, China. Environ. Sci. Pollut. Res. 28 (25), 33491–33504. https://doi.org/10.1007/s11356-021-12987-7.
Mara, S., Tanasescu, M., Ozunu, A., Vlad, S.N., 2007. Criteria for identifying the major risks associated with tailings ponds in Romania. Mine Water Environ. 26 (4), 256–263. https://doi.org/10.1007/s10230-007-0018-0.
Nakagawa, K., Yu, Z.-Q., Berndtsson, R., Hosono, T., 2020. Temporal characteristics of groundwater chemistry affected by the 2016 Kumamoto earthquake using self-organizing maps. J. Hydrol. 582, 124519 https://doi.org/10.1016/j.jhydrol.2019.124519.
Peša, I., 2021. Between waste and profit: environmental values on the Central African Copperbelt. Extractive Ind. Soc. 8 (4), 100793. https://doi.org/10.1016/j.exis.2020.08.004.
Qi, Y., Wei, X., Zhao, M., Pan, W., Jiang, C., Wu, J., Li, W., 2022. Heavy metal pollution characteristics and potential ecological risk assessment of soils around three typical antimony mining areas and watersheds in China. Front. Environ. Sci. 10 https://doi.org/10.3389/fenvs.2022.913293.
Qi, C., Wu, F., Deng, Q., Liu, G., Mo, C., Liu, B., Zhu, J., 2011. Distribution and accumulation of antimony in plants in the super-large Sb deposit areas, China. Microchem. J. 97 (1), 44–51. https://doi.org/10.1016/j.microc.2010.05.016.
Qing, X., Yutong, Z., Shenggao, L.u., 2015. Assessment of heavy metal pollution and human health risk in urban soils of steel industrial city (Anshan), Liaoning, Northeast China. Ecotoxicol. Environ. Saf. 120, 377–385. https://doi.org/10.1016/j.ecoenv.2015.06.019.
Rashed, M.N., 2010. Monitoring of contaminated toxic and heavy metals, from mine tailings through age accumulation, in soil and some wild plants at Southeast Egypt. J. Hazard. Mater. 178 (1-3), 739–746. https://doi.org/10.1016/j.jhazmat.2010.01.147.
Rehman, M.Z.u., Rizwan, M., Hussain, A., Saqib, M., Ali, S., Sohail, M.I., Shafiq, M., Hafeez, F., 2018. Alleviation of cadmium (Cd) toxicity and minimizing its uptake in wheat (Triticum aestivum) by using organic carbon sources in Cd-spiked soil. Environ. Pollut. 241, 557–565. https://doi.org/10.1016/j.envpol.2018.06.005.
Ren, B., Wang, Q., Chen, Y., Ding, W., Zheng, X., 2015. Analysis of the metals in soil-water interface in a manganese mine. J. Anal. Methods Chem. 2015, 163163 https://doi.org/10.1155/2015/163163.
Sheng, L., Hao, C., Guan, S., Huang, Z., 2022. Spatial distribution, geochemical behaviors and risk assessment of antimony in rivers around the antimony mine of Xikuangshan, Hunan Province, China. Water Sci Technol. 85 (4), 1141–1154. https://doi.org/10.2166/wst.2022.030.
Sun, R., Gao, Y., Xu, J., Yang, Y., Zhang, Y., Mohanty, K., 2021. Contamination features and source apportionment of heavy metals in the river sediments around a lead-zinc mine: a case study in Danzhai, Guizhou, China. J. Chem. 2021, 1–11. https://doi.org/10.1155/2015/163163.
Sutherland, R.A., 2000. Bed sediment-associated trace metals in an urban stream, Oahu, Hawaii. Environ. Geol. 39 (6), 611–627. https://doi.org/10.1007/s002540050473.
Wang, J., Zhang, X.-X., Chen, A.-F., Wang, B., Zhao, Q.-B., Liu, G.-N., Xiao, X., Cao, J.-N., 2022. Source analysis and risk evaluation of heavy metal in the sediment of polymetallic mining area: taking the skarn type Cu-Fe-Au deposit of Tonglüshan as an example, Hubei Province, China. China Geol. 5, 1–13. https://doi.org/10.31035/cg2022052.
Wen, W., Zhao, H., Ma, J., Li, Z., Li, H., Zhu, X., Shao, J., Yang, Z., Yang, Y., He, F., Liu, Y., 2018. Effects of mutual intercropping on Pb and Zn accumulation of accumulator plants Rumex nepalensis, Lolium perenne and Trifolium repens. Chem. Ecol. 34 (3), 259–271. https://doi.org/10.1080/02757540.2018.1427229.
Wu, F., Fu, Z., Liu, B., Mo, C., Chen, B., Corns, W., Liao, H., 2011. Health risk associated with dietary co-exposure to high levels of antimony and arsenic in the world's largest antimony mine area. Sci. Total Environ. 409 (18), 3344–3351. https://doi.org/10.1016/j.scitotenv.2011.05.033.
Wu, H., Xu, C., Wang, J., Xiang, Y., Ren, M., Qie, H., Zhang, Y., Yao, R., Li, L., Lin, A., 2021. Health risk assessment based on source identification of heavy metals: a case study of Beiyun River, China. Ecotoxicol. Environ. Saf. 213, 112046 https://doi.org/10.1016/j.ecoenv.2021.112046.
Xia, X., Yang, Z., Yu, T., Zhang, C., Hou, Q., 2019. Predicting spatial and temporal variation of Cd concentration in rice grains in the Lower Changjiang Plain during 2004–2014 based on soil geochemical survey data with GIS. J. Geochem. Explor. 200, 276–283. https://doi.org/10.1016/j.gexplo.2018.08.004.
Xia, F., Zhang, C., Qu, L., Song, Q., Ji, X., Mei, K., Dahlgren, R.A., Zhang, M., 2020. A comprehensive analysis and source apportionment of metals in riverine sediments of a rural-urban watershed. J. Hazard. Mater. 381, 121230 https://doi.org/10.1016/j.jhazmat.2019.121230.
Xiang, L., Liu, P.-H., Jiang, X.-f., Chen, P.-J., 2019. Health risk assessment and spatial distribution characteristics of heavy metal pollution in rice samples from a surrounding hydrometallurgy plant area in No. 721 uranium mining, East China. J. Geochem. Explor. 207, 106360 https://doi.org/10.1016/j.gexplo.2019.106360.
Xiao, R., Guo, D.i., Ali, A., Mi, S., Liu, T., Ren, C., Li, R., Zhang, Z., 2019. Accumulation, ecological-health risks assessment, and source apportionment of heavy metals in paddy soils: a case study in Hanzhong, Shaanxi, China. Environ. Pollut. 248, 349–357. https://doi.org/10.1016/j.envpol.2019.02.045.
Xiao, H., Shahab, A., Xi, B., Chang, Q., You, S., Li, J., Sun, X., Huang, H., Li, X., 2021. Heavy metal pollution, ecological risk, spatial distribution, and source identification in sediments of the Lijiang River, China. Environ. Pollut. 269, 116189 https://doi.org/10.1016/j.envpol.2020.116189.
Xiao, M., Xu, S., Yang, B., Zeng, G., Qian, L., Huang, H., Ren, S., 2022. Contamination, Source apportionment, and health risk assessment of heavy metals in farmland soils surrounding a typical copper tailings pond. Int. J. Environ. Res. Public Health 19 (21), 14264. https://doi.org/10.3390/ijerph192114264.
Xie, Q., Ren, B., 2022. Pollution and risk assessment of heavy metals in rivers in the antimony capital of Xikuangshan. Sci. Rep. 12 (1), 14393 https://doi.org/10.1038/s41598-022-18584-z.
Yang, R., Li, Z., Huang, B., Luo, N., Huang, M., Wen, J., Zhang, Q., Zhai, X., Zeng, G., 2018. Effects of Fe(III)-fulvic acid on Cu removal via adsorption versus coprecipitation. Chemosphere 197, 291–298. https://doi.org/10.1016/j.chemosphere.2018.01.042.
Yang, Z., Zhang, Z., Chai, L., Wang, Y., Liu, Y.i., Xiao, R., 2016. Bioleaching remediation of heavy metal-contaminated soils using Burkholderia sp. Z-90. J. Hazard. Mater. 301, 145–152. https://doi.org/10.1016/j.jhazmat.2015.08.047.
Yin, Z., 2023. The pollution of microplastics in sediments: The ecological risk assessment and pollution source analysis. Sci. Total Environ. 859 (Pt 2), 160323 https://doi.org/10.1016/j.scitotenv.2022.160323.
Yong, J., Liu, Q., Wu, B., Chen, H., Feng, G., Hu, Y., 2021. Measurement and spatial distribution pattern of natural radioactivity in a uranium tailings pond in Northwest China. J. Radiat. Res. Appl. Sci. 14 (1), 344–352. https://doi.org/10.1080/16878507.2021.1964314.
Young, G., Chen, Y., Yang, M., 2021. Concentrations, distribution, and risk assessment of heavy metals in the iron tailings of Yeshan National Mine Park in Nanjing, China. Chemosphere 271, 129546. https://doi.org/10.1016/j.chemosphere.2021.129546.
Yuan, H., Song, S., An, S., Liu, E., 2018. Ecological risk assessment of potentially toxic elements (PTEs) in the soil-plant system after reclamation of dredged sediment. Environ. Sci. Pollut. Res. Int. 25 (29), 29181–29191. https://doi.org/10.1007/s11356-018-2950-x.
Zhang, Z., Wang, J.J., Ali, A., DeLaune, R.D., 2016. Heavy metals and metalloid contamination in Louisiana Lake Pontchartrain Estuary along I-10 Bridge. Transp. Res. Part D: Transp. Environ. 44, 66–77. https://doi.org/10.1016/j.trd.2016.02.014.

Zhang, H., Zhang, Z., Ma, X., Zhang, Q., 2021. Spatial distribution and risk assessment of pollutants in a tailings pond for gold mining in Pinggu District, Beijing, China. Environ. Earth Sci. 80 (11) https://doi.org/10.1007/s12665-021-09710-7.

Zhao, G., Ding, W., Tian, J., Liu, J., Gu, Y., Shi, S., Wang, R., Sun, N., 2022. Spearman rank correlations analysis of the elemental, mineral concentrations, and mechanical parameters of the Lower Cambrian Niutitang shale: a case study in the Fenggang block, Northeast Guizhou Province, South China. J. Pet. Sci. Eng. 208, 109550. https://doi.org/10.1016/j.petrol.2021.109550.

Zhu, D., Wei, Y., Zhao, Y., Wang, Q., Han, J., 2018. Heavy Metal Pollution and Ecological Risk Assessment of the Agriculture Soil in Xunyang Mining Area, Shaanxi Province, Northwestern China. Bull. Environ. Contam. Toxicol. 101 (2), 178–184. https://doi.org/10.1007/s00128-018-2374-9.